APPLIED AND ENVIRONMENTAL MICROBIOLOGY, Oct. 2010, p. 6664–6672 Vol. 76, No. 19
0099-2240/10/$12.00 doi:10.1128/AEM.00662-10

Polyphasic Characterization of a Thermotolerant Siderophilic Filamentous Cyanobacterium That Produces Intracellular Iron Deposits▽†

Igor I. Brown,[1]* Donald A. Bryant,[2] Dale Casamatta,[3] Kathie L. Thomas-Keprta,[1] Svetlana A. Sarkisova,[1] Gaozhong Shen,[2] Joel E. Graham,[2]§ Eric S. Boyd,[4] John W. Peters,[4] Daniel H. Garrison,[1] and David S. McKay[5]

Jacobs Engineering/NASA Johnson Space Center, JE 23, P.O. Box 58447, Houston, Texas 77258-8447[1]; Department of Biochemistry and Molecular Biology, The Pennsylvania State University, University Park, Pennsylvania 16802[2]; Department of Biology, University of North Florida, Jacksonville, Florida 32224[3]; Department of Chemistry and Biochemistry and The Astrobiology Biogeocatalysis Research Center, Montana State University, Bozeman, Montana 59717[4]; and NASA Johnson Space Center, KR, 2101 NASA Parkway, Houston, Texas 77058[5]

Received 16 March 2010/Accepted 1 August 2010

Despite the high potential for oxidative stress stimulated by reduced iron, contemporary iron-depositing hot springs with circum-neutral pH are intensively populated with cyanobacteria. Therefore, studies of the physiology, diversity, and phylogeny of cyanobacteria inhabiting iron-depositing hot springs may provide insights into the contribution of cyanobacteria to iron redox cycling in these environments and new mechanisms of oxidative stress mitigation. In this study the morphology, ultrastructure, physiology, and phylogeny of a novel cyanobacterial taxon, JSC-1, isolated from an iron-depositing hot spring, were determined. The JSC-1 strain has been deposited in ATCC under the name *Marsacia ferruginose*, accession number BAA-2121. Strain JSC-1 represents a new operational taxonomical unit (OTU) within *Leptolyngbya* sensu lato. Strain JSC-1 exhibited an unusually high ratio between photosystem (PS) I and PS II, was capable of complementary chromatic adaptation, and is apparently capable of nitrogen fixation. Furthermore, it synthesized a unique set of carotenoids, but only chlorophyll *a*. Strain JSC-1 not only required high levels of Fe for growth (≥40 μM), but it also accumulated large amounts of extracellular iron in the form of ferrihydrite and intracellular iron in the form of ferric phosphates. Collectively, these observations provide insights into the physiological strategies that might have allowed cyanobacteria to develop and proliferate in Fe-rich, circum-neutral environments.

Cyanobacteria inhabiting ferrous iron-rich hot springs with circum-neutral pH represent unique models for examining the mechanisms by which early organisms evolved to cope with such habitats common on early Earth. Such organisms have previously been shown to be resistant to Fe^{2+} (37) or Fe^{3+} (6, 7) at concentrations in the micromolar to millimolar range. Moreover, high Fe concentrations (apparent optimum of ~0.5 mM) stimulated the growth of these cyanobacteria, which were described as siderophilic (having an affinity for iron) cyanobacteria (7).

The cyanobacteria inhabiting the Chocolate Pots hot springs in Yellowstone National Park, Wyoming, were shown to have played at least a passive role in contributing to iron deposition by serving as nucleation sites for the accumulation of iron minerals and associated silica deposits (36, 38). The precipitation of external iron that encrusts the cyanobacterial cells inhabiting this hot spring appears to be dependent on the species composition and chemistry of the mat (36, 38); however, multiple anoxygenic phototrophs found in the Chocolate Pots hot springs (8) could also contribute to the formation of Fe oxides (21, 49). Therefore, only iron mineralization experiments with model cyanobacterial strains can demonstrate the role of siderophilic cyanobacteria in the formation of specific, iron-bearing minerals.

An additional common feature of circum-neutral iron-depositing hot springs is elevated concentrations of hydrogen peroxide (50). Shcolnick and coauthors (41) showed that a wild type of *Synechococcus* sp. PCC 6803 was resistant to 8 mM H_2O_2 if grown with 0.3 μM Fe^{3+}, while the same concentration of hydrogen peroxide completely inhibited the growth of this cyanobacterium if it was grown with 10 μM Fe^{3+}. If a similar correlation between iron concentration and the magnitude of an externally applied oxidative stress were the case for siderophilic cyanobacteria, iron-depositing hot springs should be free of cyanobacteria. However, such springs are very rich with cyanobacteria (38, 7, 36), which suggests that siderophilic cyanobacteria may possess unusual mechanisms of iron homeostasis maintenance and oxidative stress mitigation. Additionally, understanding iron tolerance and phenomena associated with siderophily in oxygenic prokaryotes is also important because such siderophilic organisms might help us find applications for bioremediation of waters polluted with iron.

* Corresponding author. Mailing address: Jacobs Engineering/NASA Johnson Space Center, JE 23, P.O. Box 58447, Houston, TX 77258-8447. Phone: (281) 636-7609. Fax: (832) 284-4207. E-mail: igor_brown@hotmail.com.

§ Present address: Center for Marine Biotechnology, University of Maryland Biotechnology Institute, Baltimore, MD 21202.

† Supplemental material for this article may be found at http://aem.asm.org/.

▽ Published ahead of print on 13 August 2010.

The current work describes the morphology, ultrastructure, physiology, and phylogeny of a previously undescribed, siderophilic cyanobacterium. The results of this polyphasic characterization led to the conclusion that strain JSC-1 represents a new operational taxonomic unit (OTU). (The epithet for JSC-1, *Marsacia ferruginose*, was chosen in honor of Nicole Tandeau de Marsac.) Additionally, biomineralization of intracellular iron by a cyanobacterium is demonstrated for the first time.

MATERIALS AND METHODS

Source of organism and cultivation. Samples of a floating cyanobacterial mat were collected in September 2004 from a roadside effluent channel. This channel is fed from two springs that correspond to features LDHSNN001 and LDHSNN001 in the Yellowstone National Park geothermal inventory listed at http://www.rcn.montana.edu/resources/features/features.aspx?nav=11&region=82. The concentration of Fe in the spring water sampled adjacent to the mat was ~7 μM as determined by the FerroZine method (16).

The isolation procedure, medium, and cultivation have been described previously (6). Motility in a light gradient and light microscopy are described in the supplemental material. The determination of the iron requirement and tolerance for JSC-1 was performed as described previously (6).

Electron microscopy and EDX analysis. Transmission electron microscopy (TEM) was employed to study the ultrastructure of strain JSC-1 (6). To study the internal and external Fe-bearing precipitates, ultramicrotome thin sections were analyzed by scanning TEM (STEM) and energy dispersive X ray (EDX) spectroscopy. Cells were prepared for ultramicrotomy as previously described (4), with several modifications. Briefly, cells were fixed initially with glutaraldehyde alone and were then embedded in Spurr's low-viscosity epoxy. No formaldehyde was used, and phosphate buffer was replaced with 0.2 M sodium cacodylate buffer, pH 6.5 (38). When cured, the embedded cells were sliced into sections (70 to 100 nm thick) using an RMC-Eiko MT-6000 XL microtome equipped with a 45° angle diamond knife. Individual sections were transferred to substrate-free Cu 200 mesh TEM grids and stained by using one or more heavy-metal staining agents (e.g., osmium tetroxide, uranyl acetate, and lead citrate), while some sections remained unstained to avoid overlapping the phosphorous EDX peak (Kα, 2.014 keV) with those of osmium (Mα12, 1.909 keV; Mβ, 1.978 keV). Thin sections were analyzed with a JEOL 2000 FX 200-keV STEM and/or a JEOL 2500SE 200-keV field emission STEM. These instruments were equipped with light element ($Z > 5$) Si-drift EDX detectors (Noran System 6). Mineralogical information was obtained by electron diffraction of selected areas. Quantitative two-dimensional maps were collected for elements for which 8 was $\leq Z$ and Z was ≤ 26, at a spatial resolution of <100 nm. Samples for the scanning electron microscopy (SEM) were collected on 0.45-μm-pore-diameter filters (Millipore), air-dried, coated with ~2 nm of carbon to improve electron conductivity, and visualized using a JEOL JSM-6100 SEM.

DNA extraction and amplification. A Mo-Bio extraction kit (UltraClean microbial DNA isolation kit; Mo Bio Laboratories, Inc.) was used for DNA extraction per the manufacturer's instructions. PCR products were cloned to identify nonidentical ribosomal sequences; 12 transformant colonies were selected for full-length sequencing of the cloned 16S rRNA amplicons from the JSC-1 strain. The nearly complete 16S to 23S rRNA intergenic spacer region was amplified with custom primers p381798 (5′-TGG CGG TAT GCT TAA C-3′) and p381799R (5′-TCG GGC TAC TAA GAT G-3′) with the following PCR components: 5 μl 10× PCR buffer, 1.75 μl 10 mM dNTPs, 0.5 μl 25 mM $MgCl_2$, 2 μl 25 ng/μl genomic DNA, 2 μl 5 μM each primer, 0.75 μl 5 U/μl enzyme mix (Roche Applied Science, Indianapolis, IN), and nuclease-free water added to a final volume of 50 μl. PCRs were conducted in a Hybaid thermal cycler with an initial denaturing step at 95°C for 2 min; 9 cycles of 95°C for 10 s, 55°C for 30 s, 68°C for 8 min; 24 cycles of 95°C for 15 s, 55°C for 30 s, 68°C for 8 min (+20 s/cycle); and a final elongation step at 68°C for 7 min.

Purified PCR products were cloned with a TOPO TA cloning kit (Invitrogen, Carlsbad, CA) with an extended incubation of 30 min and transformed into ElectroMAX DH10B T1 phage-resistant competent cells (Invitrogen). Plasmids were purified with the CosMCPrep template purification system (Agencourt Bioscience Corporation) and bidirectionally sequenced on an ABI3730XL DNA analyzer (Applied Biosystems, Foster City CA). The resulting sequences were assembled using Phred and Phrap and were analyzed with Consed (18).

Phylogenetic methods. ChromasPro (Technelysium Pty Ltd., Tewantin QLD, Australia) was used to combine and edit all sequence data. The 16S sequence of the new strain was combined with 16S rRNA sequences from GenBank designated *Leptolyngbya*, and sequences from any taxa that showed ≥97.5% sequence similarity via BLASTn searches were included. The sequences were aligned by using the ClustalX Web interface (27) and manually checked and edited by using Maclade version 4.06 (28). Maximum parsimony (MP) trees were generated by using a heuristic search and constrained by a random sequence addition (of 1,000), steepest descent and tree bisection, and reconnection branch swapping (tree bisection-reconnection) with PAUP version 4.02b (45). Bootstrap values were obtained from 1,000 replicates with 1 random sequence addition to jumble the data. A maximum likelihood (ML) tree was constructed with 100 rounds (each with its own random addition) by using the general time-reversible model with corrected invariable sites (I) and a gamma distribution-shaped parameter (G). Trees based on ML and MP were generated from these data using PAUP version 4.02 running 1,000 replicates of each. Sequence similarities were calculated online with ClustalW at http://www.ebi.ac.uk/clustalw/index.html.

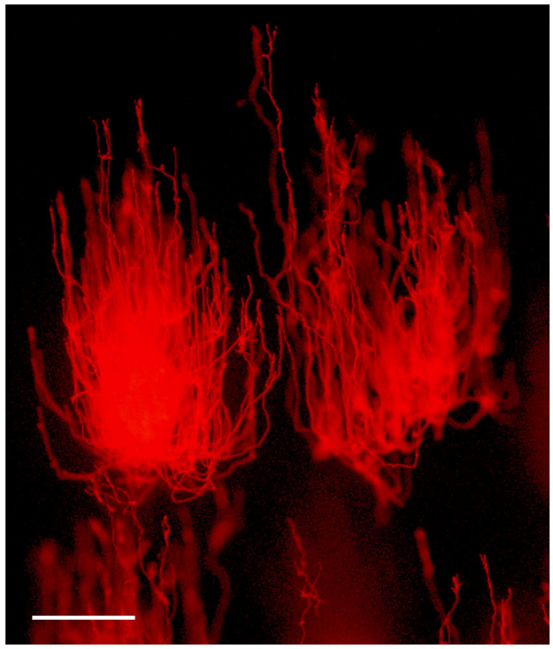

FIG. 1. Photomicrograph illustrating swarming migration of JSC-1 clusters to a light source on semisolid medium. DH medium was solidified with 0.9% agarose and supplemented with 40 μM $FeCl_3 \cdot 6H_2O$. Light source was located at the top. Epifluorescent microscopy was used to visualize JSC-1 filaments. Bar = 500 μm.

Isolation of phycobiliproteins, and absorption and fluorescence spectroscopy. Phycobilisomes (PBS) were isolated from JSC-1 cells as described previously (10). For further analysis, different phycobiliproteins of JSC-1 phycobilisomes (PBSs) were partly separated by DEAE cellulose ion-exchange column chromatography, and fractions were compared by absorption and fluorescence spectroscopy. Absorption spectra of whole cells and purified phycobiliproteins were measured with a GENESYS 10 spectrophotometer (Thermo Spectronic, Rochester, NY). Fluorescence emission spectra were measured with an SLM 8000C spectrofluorometer described previously (42). The excitation wavelength was 350 nm for excitation of phycoerythrin and 590 nm for preferential excitation of phycocyanin and allophycocyanin. For chlorophyll-protein complexes, 440-nm excitation was used. For measuring low-temperature fluorescence emission spectra, samples were diluted in 25 mM HEPES-NaOH, pH 7, with 60% (vol/vol) glycerol before freezing in liquid nitrogen. Spectral data were processed and analyzed by using the data processing program IGOR Pro (WaveMetrics Inc., Lake Oswego, OR).

RESULTS

Morphology and ultrastructure. JSC-1 was isolated from an environment with a temperature of ~45°C. After 3 days incubation above 65°C, these cells remained viable (not shown). Therefore, JSC-1 can thus be classified as a thermotolerant

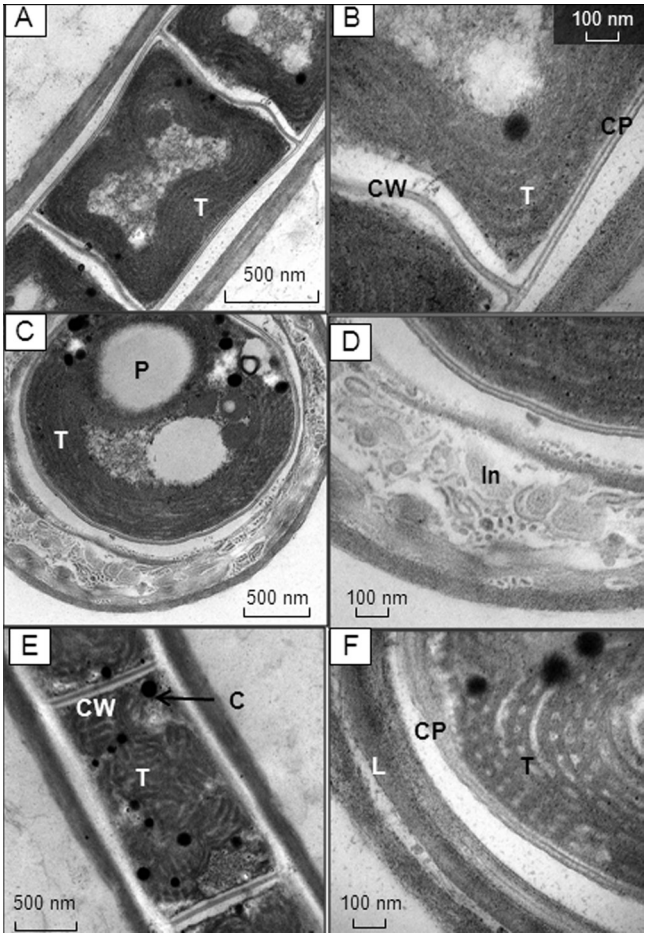

FIG. 2. TEM micrographs of JSC-1 cells grown with 40 μM $FeCl_3 \cdot 6H_2O$. (A to D) Sections of isodiametric cells; (E and F) sections of elongated cells; (A, B, and E) longitudinal sections; (C, D, and F) cross sections. T, thylakoids; CP, cytoplasmic membrane; CW, cross wall; P, polyphosphate body; In, inclusions within external sheath; C, cyanophycin granules.

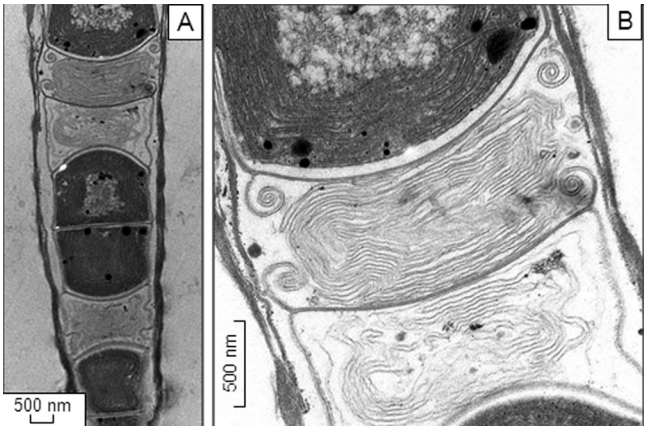

FIG. 3. TEM micrographs of a necridial cells (longitudinal section) shown under different magnifications (A and B). Note the presence of membrane-like patterns within necredial cells.

organism (29). Filaments were ~500 to 2,500 μm in length, with multiple loops and reversions (see Fig. S1A and D in the supplemental material) even under conditions that stimulated phototactic movement (Fig. 1). Multiple granules in cells (see Fig. S1A and B), necridial cells (see Fig. S1A and B), and detached sheaths (see Fig. S1D) were all visible. JSC-1 filaments terminated with a rounded apical cell (see Fig. S1E).

Two morphotypes were observed in the JSC-1 culture (see Table S1 in the supplemental material). The first morphotype had almost isometric cells with an average length of 2.52 ± 0.41 μm, width of 2.16 ± 0.13 μm, and a length-to-width (L/W) ratio of ~1.17. The second morphotype had slightly elongated cylindrical cells with a length of 2.89 ± 0.27 μm, width of 1.62 ± 0.17 μm, and a length/width ratio of 1.78. Similar cellular heterogeneity was reported earlier for *Leptolyngbya frigida* ANT.LH70.1 (32), a distant relative of strain JSC-1 (see "Phylogeny"). False branching of JSC-1 filaments was not observed. Strain JSC-1 produced hormogonia in the stationary phase or under P limitation (data not shown).

TEM studies showed that the cross walls in JSC-1 were approximately 22 nm thick, and neither junctions nor cytoplasmic membrane pores were observed (Fig. 2A and B). However, two basic patterns for thylakoid membranes were detected (Fig. 2B and F). Transverse and cross sections of short cells demonstrated a peripheral but undulating alignment of thylakoids relative to the internal side of the cytoplasm membranes of the cells (Fig. 2A to C), with five to six thylakoids per cell observed on average. For elongated cells, the thylakoid membranes assembled into a more irregular pattern, described as a knit-ball structure (Fig. 2E and F).

The sheaths of JSC-1 were colorless, thick, persistent, firm, and easily visible by both light microscopy (see Fig. S1A and B in the supplemental material) and TEM (Fig. 2C, D, and F). In contrast to the persistent, nonlaminated sheaths typically observed for *Leptolyngbya* (14), the sheaths of JSC-1 cells were laminated (Fig. 2C, D, and F). Detailed TEM analysis revealed very tiny bodies within the sheath (Fig. 2D) not observed in other representatives of *Leptolyngbya*. The necridia were filled with symmetrical membrane patterns (Fig. 3A and B) with no chlorophyll autofluorescence (see Fig. S1C).

Motility and phototaxis. When cultivated on semisoft DH medium (14a) solidified with 0.8% (wt/vol) SeaKem agarose (BioWhitaker Molecular Applications) under a gradient of light, JSC-1 was capable of disseminating on the surface and inside a soft gel by generation of "swarms or aggregate of hundreds or thousands of trichomes" (12) that moved toward a light source (Fig. 1). Single swarms of strain JSC-1, the so-called puff morphology (39), were also observed with liquid culture (data not shown). Filaments also exhibited upright aerial growth (see Fig. S2 in the supplemental material).

Phylogeny. Because the MP and ML trees were largely congruent, only the ML tree is presented (Fig. 4). The 16S rRNA sequence of JSC-1 clustered with *Leptolyngbya* sp. Kovacik 1999/1 (GQ495618), *L. frigida* Ant.LH70.1 (AY493574), *Leptolyngbya* sp. CENA 112 (EF088337), and CENA 103 (EF088339), but not with *L. frigida* ANT.LH52.2 (AY493575) (Fig. 4). However, the 16S rRNA sequence of strain JSC-1 was <95% identical to these closest relatives. Strain JSC-1, reference *Leptolyngbya* sp. PCC 6306 for cluster 1 (14) and *Leptolyngbya boryana* sp. PCC 73110, which is frequently used as a

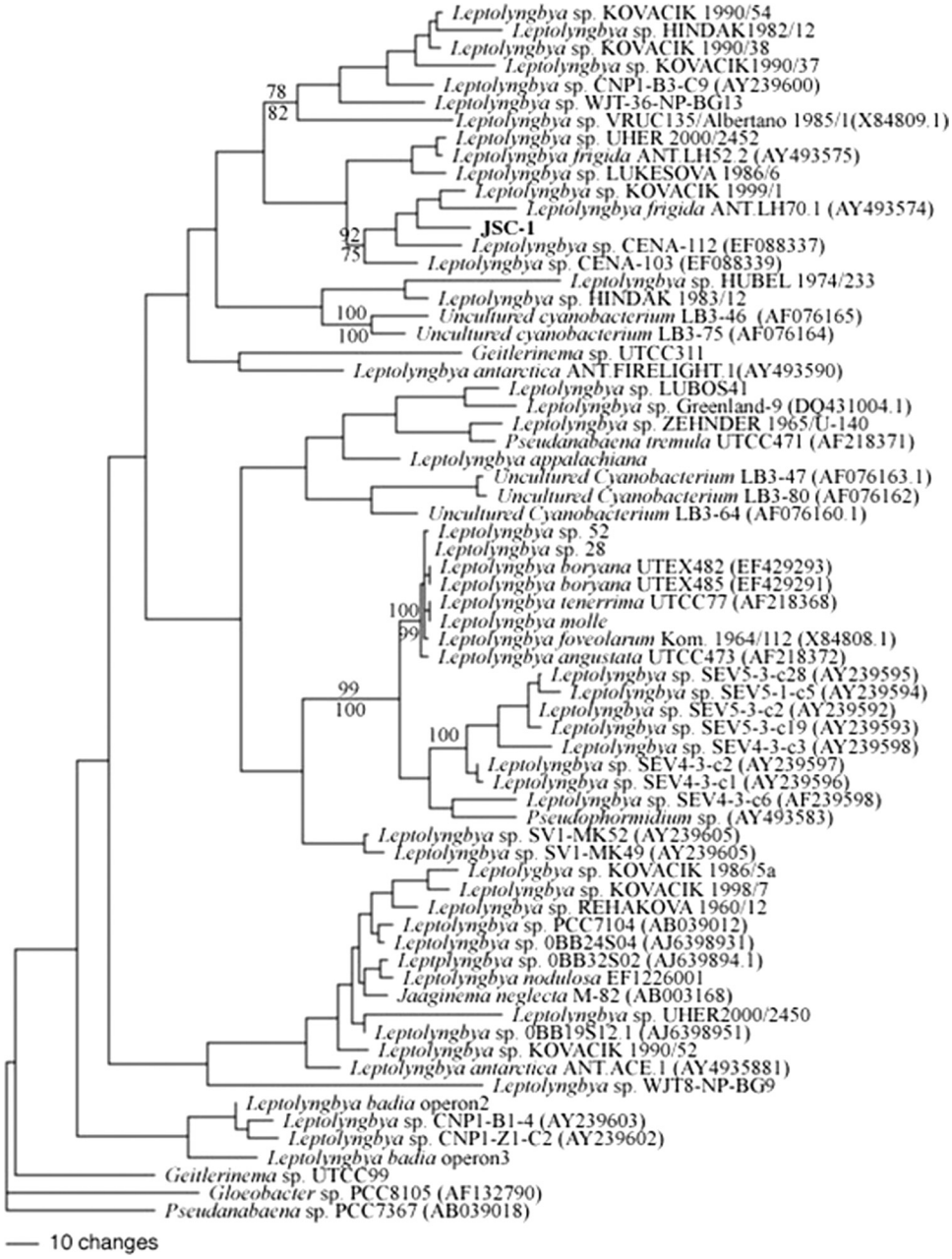

FIG. 4. Maximum likelihood tree for JSC-1 based on 16S rRNA gene sequences (1,050 bp). Accession numbers are given in parentheses. Numbers at nodes indicate bootstrap support (MP values above nodes; ML below).

reference strain for the *Leptolyngbya* group (30, 46, 47), did not demonstrate coclustering (Fig. 4). These results suggest that JSC-1 is a representative of a new genus-level OTU aligned with *Leptolyngbya* sp. Kovacik 1999/1 (22), *L. frigida* Ant.LH70.1 (46, 47), and *Leptolyngbya* spp. CENA 112 and CENA 103 (17). The *nifH* gene was also detected in JSC-1 by PCR amplification, although the high degree of sequence conservation in the amplified region made it difficult to resolve its phylogenetic affiliation (see Fig. S3 in the supplemental material).

Stoichiometry of the photosystems and pigment composition. To investigate the chlorophyll-protein composition in JSC-1 cells, low-temperature fluorescence emission spectra were measured on whole cells (data not shown) and on the isolated thylakoid membranes (Fig. 5A). The fluorescence emission maximum derived from chlorophylls associated with photosystem (PS) I occurred at 725 nm for JSC-1 thylakoids but occurs at 715 nm for *Synechococcus* sp. PCC 7002; PS II-associated chlorophylls contributed fluorescence emission peaks at 685 and 695 nm, respectively (42, 51). The relative amplitude of fluorescence emission from PS I was significantly larger than that from PS II in JSC-1 cells. Based on a comparison of the fluorescence emission amplitudes for membranes at equal chlorophyll content, the PS I/PS II ratio (~3.7) in the

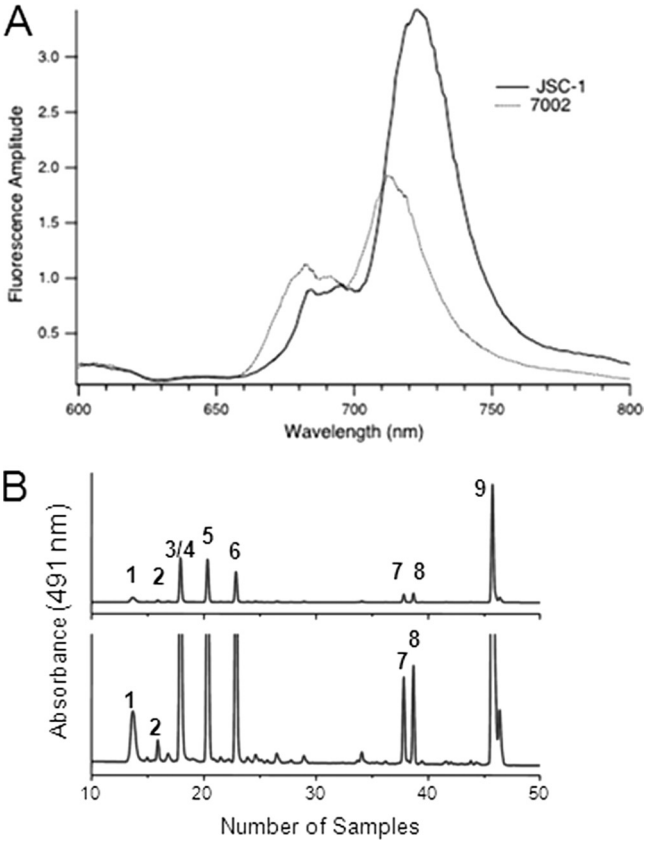

FIG. 5. Characterization of JSC-1 pigment composition. (A) Comparison of 77K fluorescence emission spectra measured for isolated thylakoid membranes from JSC-1 and *Synechococcus* sp. PCC 7002. Thylakoids were adjusted to equal Chl concentrations (5 μg/ml). The excitation wavelength was 440 nm, and each spectrum is the average of four individual measurements. (B) HPLC chromatogram of methanolic extract of JSC-1 cells. Top panel, full scale; bottom panel, magnification, ×10. Compounds are as follows: 1, synechoxanthin; 2, 2-hydroxy-myxoxanthophyll; 3, myxoxanthophyll (myxol-2′-fucoside); 4, nostaxanthin; 5, caloxanthin; 6, zeaxanthin; 7, cryptoxanthin; 8, echinenone; 9, β-carotene.

JSC-1 thylakoid membranes is about twice the PS I/PS II ratio (~1.8) measured for thylakoid membranes of *Synechococcus* sp. PCC 7002.

Fractions enriched in various phycobiliproteins were produced from isolated phycobilisomes (11) by ion-exchange chromatography and were analyzed by absorption and fluorescence emission spectroscopy (data not shown). The data suggest that strain JSC-1 synthesizes three major phycobiliproteins: phycoerythrin, phycocyanin, and allophycocyanin. A preliminary analysis of the incomplete draft genome indicated that strain JSC-1 should be capable of type III chromatic adaptation (R. M. Alvey and D. A. Bryant, unpublished observations).

Carotenoids were analyzed by high-performance liquid chromatography (HPLC), and nine carotenoids were detected: synechoxanthin, 2-hydroxy-myxoxanthophyll, myxoxanthophyll (myxol-2′-fucoside), nostaxanthin, caloxanthin, zeaxanthin, cryptoxanthin, echinenone, and β-carotene (Fig. 5B). The only chlorophyll detected was Chl *a* esterified with phytol.

Iron tolerance and iron mineralization. JSC-1 cells were inoculated in DH medium (pH 8.2) with a range of Fe^{3+} concentrations of up to 10 mM. JSC-1 slightly grew in DH medium without added Fe^{3+} during the 10 days after inoculation and did not decompose during a subsequent 10-day period (see Fig. S4 in the supplemental material, solid line). In contrast, *Synechocystis* sp. PCC 6803 decomposed very quickly after inoculation in DH medium without added Fe^{3+} (data not shown). The relative stability of JSC-1 in an iron-deficient medium led to the hypothesis that JSC-1 is able to accumulate iron within cells. As measured (31) by increasing Chl *a* concentration, JSC-1 growth increased with increasing concentrations up to 1,000 μM (see Fig. S4 in the supplemental material); however, 5 to 10 mM $FeCl_3 \cdot 6H_2O$ was toxic for JSC-1 as well as other siderophilic cyanobacteria (data not shown).

When JSC-1 was grown in DH medium supplemented with $FeCl_3 \cdot 6H_2O$, the filaments, averaging ~3 μm in diameter, were coated with Fe-rich nanoparticles, with the thickness of the coating ranging from a few nanometers to ~0.5 μm (Fig. S5A and B in the supplemental material). These coatings were composed primarily of amorphous Fe oxides (see Fig. S6A in the supplemental material). The predominant mineralogy of the Fe-rich extracellular coating is consistent with ferrihydrite ($Fe_5HO_8 \cdot 4H_2O$), while the needle-shaped Fe oxides have lattice spacings and external morphologies consistent with goethite (α-FeOOH) (data not shown). Discrete, structurally amorphous intracellular Fe-bearing precipitates with quasi-circular shapes ranging from ~40 to 200 nm in diameter were observed within some cells (Fig. 6A, black box and insert). Most cells contained only one example of these Fe-rich precipitates; however, some cells contained two Fe-rich precipitates. These Fe-rich particles typically displayed a smooth texture, although some appeared to have a texture similar to that of the external Fe-bearing precipitates (Fig. 6A, insert). The major components of the internal particles were Fe and P, although Al and Ca were also detected (Fig. 6B). Compositional differences between the external and internal Fe-bearing precipitates within a single cyanobacterial cell are shown by K-line element maps for Fe, P, Al, and Ca (see Fig. S6 in the supplemental material). Elements Fe, P, Al, and Ca appear to be associated with small satellites composed mainly of P, Ca, and O (Fig. 6B).

DISCUSSION

Morphological and ultrastructural observations clearly suggest that strain JSC-1 belongs to subsection III (formerly *Oscillatoriales*) of the *Cyanobacteria* (13, 24). A comparison of JSC-1 cell dimensions with those for different *Leptolyngbya* strains suggested that JSC-1 is unambiguously different from the morphospecies described in Table S1 in the supplemental material. The most critical morphological differences from *Leptolyngbya* sensu lato (2, 25) are the absence of any central pore in cross walls, nonparietal position of thylakoids, and the presence of firm, nonfacultatively layered sheaths. The occurrence of two types of thylakoid patterns in cells of one organism has been reported previously (34). Similar thylakoid-like membranes in necridial cells of *Leptolyngbya* sp. strain VRUC184 have been documented previously (9). The presence of necridia in JSC-1 filaments suggests that this strain

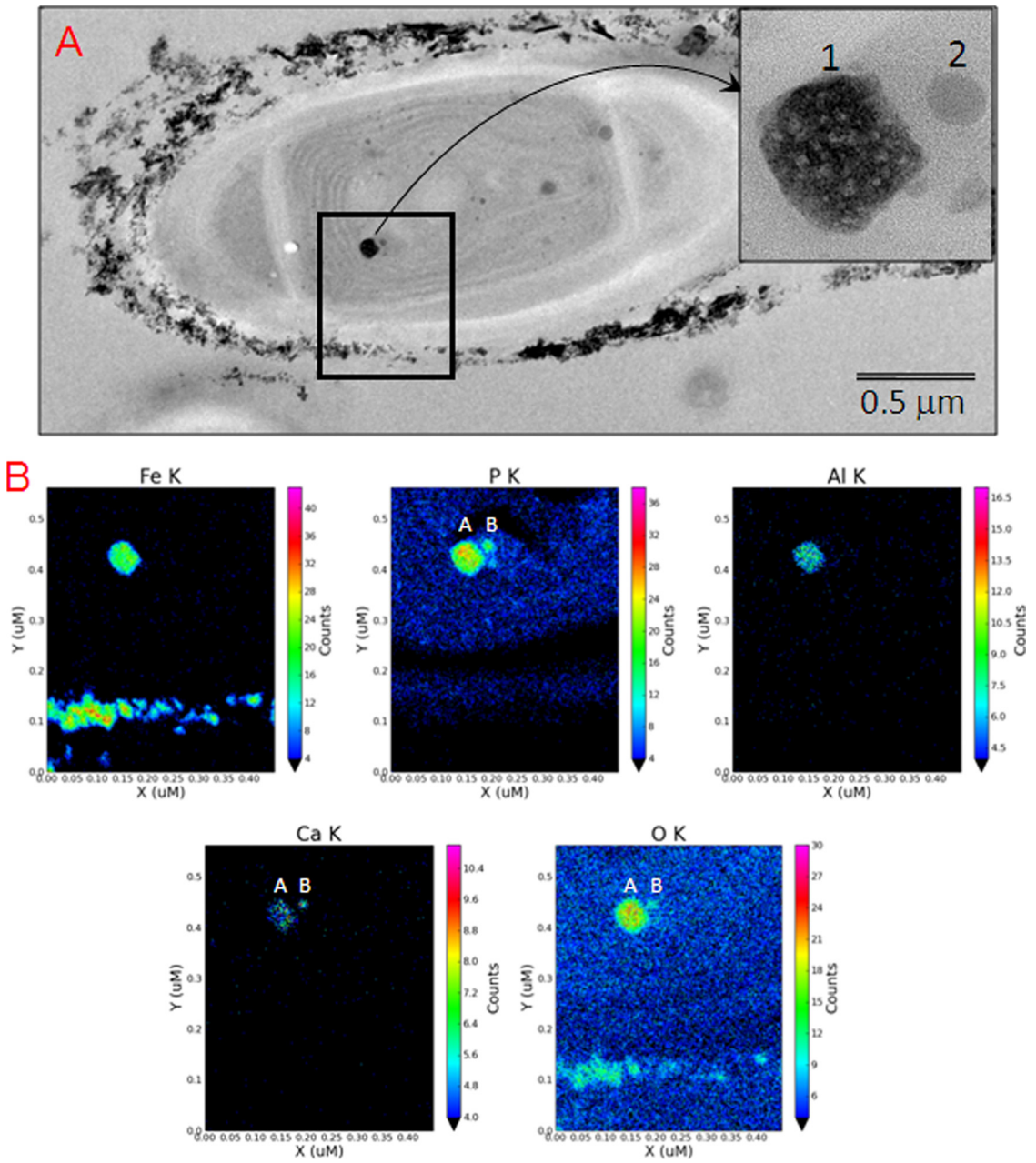

FIG. 6. TEM views of extracellular and intracellular iron-rich particles found in JSC-1 cells incubated with 600 μM $FeCl3 \cdot 6H_2O$ and 0.04 mM $Na_2HPO_4 \cdot 7H_2O$. These cells were not stained with Os. (A) TEM view of a JSC-1 cell encrusted with external Fe-bearing precipitates and containing an electron-dense, internal, Fe-rich particle ~100 nm in size (insert, image numbered 1) and a satellite body ~30 nm in size (insert, image numbered 2). (B) Quantitative element maps for internal and external particles show distribution patterns for Fe, P, Al, Ca, and O. The electron dense particle 1 contains major amounts of Fe, P, and O with minor amounts of Al and Ca. Particle 2 contains P, Ca, and O, with no detectable Fe (color panels).

might be useful for studying programmed cell death in cyanobacteria because necridia occur as areas of cell apoptosis and disintegration (26).

The swarming motility of JSC-1 is different from that of *Pseudanabaena galeata* (12). While the heads of *P. galeata* "comets" are directed to a light source, JSC-1 comets swarmed in the opposite mode: the tails, not the heads, of comets were directed to the light source (Fig. 1). Therefore, the type of phototactic motility of the JSC-1 strain increases its distinction from *Leptolyngbya* spp., which are immotile (2).

Phylogenetic analysis. The low values of similarity (<90%) to *Leptolyngbya* type strains *L. boryana* UTEX 482 and 485 and *Leptolyngbya* sp. PCC 7104 clearly placed the new isolate into a new, as yet undescribed genus (43). Furthermore, JSC-1 shares less than 97.5% sequence similarity with its closest phylogenetic relatives and can thus be considered a representative

of a new species. The clustering of the thermosiderophilic JSC-1 with ecologically disparate *Leptolyngbya* strains from Antarctica (*Leptolyngbya* sp. ANT.LH70.1), Europe (*Leptolyngbya* sp. KOVACIK 1999/1), and Brazil (*Leptolyngbya* sp. CENA 103 and 112) suggested that there are no physicochemical or geographical reasons for this clustering, while such types of clustering were observed for different groups of cyanobacteria (35) or for different *Leptolyngbya* species (9). Thus, polyphasic characterization of JSC-1 may help to reduce the number of unclassified species within *Leptolyngbya* sensu lato.

Stoichiometry of the photosystems and iron mineralization. The study of the stoichiometry of the photosystems in several siderophilic cyanobacteria suggests that the relative PS I content of JSC-1, JSC-3, and JSC-14 cells is much higher than in the well-characterized *Synechococcus* sp. strain PCC 7002 (G. Shen, D. A. Bryant, and I. I. Brown, unpublished data), and this might be observed more frequently with siderophilic cyanobacteria than with their nonsiderophilic counterparts.

Strain JSC-1 and other cyanobacteria (6, 7) found in iron-depositing hot springs require significantly higher quantities of iron for growth than their freshwater counterparts (23). Multiple experiments with iron supplementation with strain JSC-1 and other strains from iron-depositing hot springs (7) showed that these organisms are able to consume colloidal Fe^{3+}, which is probably transported into the cyanobacterial cytoplasm through an ABC-type Fe^{3+} transport system (5). Comparative analysis of regulatory mechanisms of this system in the JSC-1 strain and in nonsiderophilic thermophilic *Leptolyngbya* species seems to be a very intriguing project for a comparative genomics approach.

The stimulating effect of colloidal iron on the proliferation of siderophilic cyanobacteria (6; this study) and the accumulation of mineralized iron within the JSC-1 cytoplasm confirmed previous results that Fe^{3+} can be taken up by cyanobacteria and that they can discriminate oxidized iron concentrations (41). Thus, the decrease of Fe^{2+} concentration along an increasing oxygen gradient on the slopes of iron-depositing hot springs (e.g., the Chocolate Pots and La Duke hot springs) might not be a limiting factor for general proliferation of oxygenic phototroph communities in such environments. However, the Fe^{2+}/Fe^{3+} ratio may determine the diversity of species, identified in references 36 and 38, in defined areas of such iron-rich springs.

The mechanism that prevents oversaturation of the cyanobacterial cytoplasm with reduced iron in freshwater or marine cyanobacteria is currently being studied (see reference 41 for a review). However, it is unclear if the much-attenuated mechanisms of iron homeostasis in freshwater or/and marine cyanobacteria (3, 40) that inhabit aquatic environments with average Fe nanomolar concentration (1, 44) are sufficient to support iron homeostasis in siderophilic cyanobacteria that inhabit environments with millimolar concentrations of Fe (6, 37). One hypothesis was that siderophilic cyanobacteria could decrease the intracellular concentration of Fe^{2+} by the direct transfer of electrons from reduced iron to an e^- acceptor in the photosynthetic chain (33) and that oxidized iron should then accumulate within the cytoplasm of such siderophilic cyanobacteria in the form of a ferrihydrite (15). The high ratio of PSI/PSII observed in siderophilic cyanobacteria could provide additional support for this hypothesis. However, this study has shown for first time that oxidized iron does not accumulate as pure ferrihydrite but seems to be bound to phosphate residues or organic phosphorous-rich compounds or both. No similar features were found in iron-oxidizing anoxygenic phototrophs (21), which may point to different mechanisms for intracellular iron mineralization in siderophilic cyanobacteria. Iron-rich inclusions in JSC-1 are nearly identical to those in siderophilic strains JSC-3 and JSC-11 (K. L. Thomas-Keprta and I. I. Brown, unpublished data), having elevated ratios of PSI/PSII also. One may speculate that intracellular iron precipitation might be a common feature of siderophilic cyanobacteria with an elevated PSI/PSII ratio, but detailed studies are needed. Clearly, studies concerning the physicochemical properties of iron-rich inclusions and the molecular basis of their generation could contribute profoundly to a better understanding of adaptation mechanisms of siderophilic cyanobacteria to elevated iron and oxidative stress and to an understanding of the evolution of both processes within cyanobacteria generally. On the other hand, the absence of siderite on or within JSC-1 cells suggests that anoxygenic phototrophs rather than cyanobacteria may be the main contributors to the accumulation of iron carbonates (48) in iron-depositing hot springs.

The pigment composition. The presence of such a wide set of carotenoids may give JSC-1 some ecological advantages; e.g., the newly discovered carotenoid synechoxanthin is supposed to be a strong screen for UV-A (20), and zeaxanthin is very effective at protecting against UV-B (19). Zhu et al. (52) found that reactive oxygen species were nearly an order of magnitude higher in mutants lacking all xanthophylls than in wild-type cells after an exposure to high light intensity for 2 h. Protection of cyanobacterial cells from UV light and especially reactive oxygen species would be very important for phototrophic organisms inhabiting iron-rich springs because they would likely suffer from the generation of reactive oxygen species stimulated by high intracellular iron concentration (41).

Conclusion. The results of this study suggest that iron-depositing hot springs might be natural sanctuaries for cyanobacteria whose iron-dependent physiology seems to be more similar to putative ancestral cyanobacteria than to extant, nonsiderophilic taxa. Our preliminary analysis of siderophilic cyanobacteria diversity (7) has shown that their representatives frequently belong to new genera with novel metabolic features. Moreover, iron-depositing hot springs with circum-neutral pH are apparently very rare on Earth (35) in contrast to iron-rich acidic springs. The initial survey work on the diversity, phylogenetics, physiology, and genomics of siderophilic cyanobacteria provide justification for further studies and for the protection of current iron-depositing hot springs because of their unique scientific importance.

ACKNOWLEDGMENTS

We gratefully acknowledge support from the Astromaterials Research and Exploration Science Directorate and JSC colleagues: T. See, R. Christiansen, C. Galindo, Jr., G. A. Robinson, and M. Nelman. D.A.B. gratefully acknowledges support from National Science Foundation grant MCB-0519743 and NASA Astrobiology grant NNX09AM87G. The Astrobiology Biogeocatalysis Research

Center at Montana State University is supported by NASA Astrobiology Institute (NAI) grant NNA08C-N85A to J.W.P. E.S.B. was supported by an NAI postdoctoral fellowship.

Some preliminary results from the draft of the JSC-1 genome (JGI, DOEM_782004) were used in this article, and I.I.B. and D.A.B. are very appreciative of JGI colleagues participating in this project. I.I.B. is grateful to Beckman Coulter Genomics and to the Microscopy Center at University of Louisiana—Lafayette for exceptionally qualified service. We are grateful to four anonymous reviewers and the following colleagues for valuable suggestions: R. W. Castenholz, M. Allen, G. Guglielmi, J. A. Euzéby, and A. Oren. I.I.B. gratefully acknowledges M. Revis, J. Fairchild, M. Guevara and V. Oliva for assistance with manuscript preparation.

REFERENCES

1. **Aguilar, C., R. L. Cuhel, and J. V. Klump.** 2002. Porewater and hydrothermal vent water inputs to Yellowstone Lake, Wyoming, p. 1–18. *In* R. J. Anderson (ed.), Yellowstone Lake: hotbed of chaos or reservoir of resilience? Proceedings of the 6th Biennial Conference on the Greater Yellowstone Ecosystem. Mammoth Hot Springs, Yellowstone National Park, WY.
2. **Anagnostidis, K., and J. Komárek.** 1988. Modern approach to the classification system of Cyanophytes. 3. *Oscillatoriales.* Algol. Stud. **50–53:** 327–472.
3. **Balasubramanian, R., G. Shen, D. A. Bryant, and J. H. Golbeck.** 2006. Regulatory roles for IscA and SufA in iron homeostasis and redox stress responses in the cyanobacterium *Synechococcus* sp. strain PCC 7002. J. Bacteriol. **188:**3182–3191.
4. **Bozzola, J. J., and L. D. Russell.** 1999. Electron microscopy: principles and techniques for biologists, 2nd ed., p. 670. Jones and Bartlett Publishers, Boston, MA.
5. **Braun, V., and M. Braun.** 2004. Energy-coupled outer membrane iron transporters, p. 213–236. *In* R. Benz (ed.), Bacterial and eukaryotic porins. Wiley-VCH, Weinheim, Germany.
6. **Brown, I. I., D. Mummey, and K. E. Cooksey.** 2005. A novel cyanobacterium exhibiting an elevated tolerance for iron. FEMS Microbiol. Ecol. **52:**307–314.
7. **Brown, I., C. Allen, D. Mummey, S. Sarkisova, and D. McKay.** 2007. Iron-tolerant cyanobacteria, p. 425–442. *In* J. Seckbach (ed.), Algae and cyanobacteria in extreme environments. Springer, Dordrecht, Netherlands.
8. **Brown, I. I., S. G. Tringe, K. L. Thomas-Keprta, D. A. Bryant, S. A. Sarkisova, K. Malley, O. Sosa, C. G. Klatt, D. H. Garrison, and D. S. Mckay.** 2010. Inferring properties of ancient cyanobacteria from biogeochemical activity and genomes of siderophilic cyanobacteria, abstr. 5404. Abstr. Astrobiol. Sci. Conf. 2010.
9. **Bruno, L., D. Billi, S. Bellezza, and P. Albertano.** 2009. Cytomorphological and genetic characterization of troglobitic *Leptolyngbya* strains isolated from Roman hypogea. Appl. Environ. Microbiol. **75:**608–617.
10. **Bryant, D. A., G. Gugliemi, N. Tandeau de Marsac, A. M. Castets, and G. Cohen-Bazire.** 1979. The structure of cyanobacterial phycobilisomes: a model. Arch. Microbiol. **123:**113–127.
11. **Bryant, D. A.** 1982. Phycoerythrocyanin and phycoerythrin: properties and occurrence in cyanobacteria. J. Gen. Microbiol. **128:**835–844.
12. **Castenholz, R. W.** 1982. Motility and taxis, p. 413–439. *In* N. G. Carr and B. A. Whitton (ed.), The biology of cyanobacteria. University of California Press, Berkeley, CA.
13. **Castenholz, R. W.** 2001. General characteristics of the cyanobacteria, p. 474–487. *In* D. R. Boone and R. W. Castenholz (ed.), Bergey's manual of systematic bacteriology, 2nd ed., vol. 1. Springer-Verlag, New York, NY.
14. **Castenholz, R. W., R. Rippka, M. Herdman, and A. Wilmotte.** 2001. Form-genus V. *Leptolyngbya* Anagnostidis and Komarek 1988, p. 544–546. *In* D. R. Boone and R. W. Castenholz (ed.), Bergey's manual of systematic bacteriology, 2nd ed., vol. 1. Springer-Verlag, New York, NY.

14a. **Castenholz, R. W.** 1988. Culturing methods for cyanobacteria. Methods Enzymol. **167:**68–93.

15. **Cohen, Y.** 1989. Photosynthesis in cyanobacterial mats and its relation to the sulfur cycle: a model for microbial sulfur interactions, p. 22–36. *In* Y. Cohen and E. Rosenburg (ed.), Microbial mats: physiological ecology of benthic microbial communities. American Society for Microbiology, Washington, DC.
16. **Emerson, D., and N. P. Revsbech.** 1994. Investigation of an iron-oxidizing microbial mat community located near Aarhus, Denmark: laboratory studies. Appl. Environ. Microbiol. **60:**4032–4038.
17. **Furtado, A., M. Calijuri, A. Lorenzi, R. Honda, D. Genuário, and M. Fiore.** 2009. Morphological and molecular characterization of cyanobacteria from a Brazilian facultative wastewater stabilization pond and evaluation of microcystin production. Hydrobiologia **627:**195–209.
18. **Gordon, D.** 2003. Viewing and editing assembled sequences using Consed. Curr. Protoc. Bioinformatics **11:**Unit11.2.
19. **Gotz, T., U. Windhovel, P. Boger, and G. Sandmann.** 1999. Protection of photosynthesis against ultraviolet-B radiation by carotenoids in transformants of the cyanobacterium *Synechococcus* PCC 7942. Plant Physiol. **120:** 599–604.
20. **Graham, J. E., and D. A. Bryant.** 2008. The biosynthetic pathway for synechoxanthin, an aromatic carotenoid synthesized by the euryhaline, unicellular cyanobacterium *Synechococcus* sp. strain PCC 7002. J. Bacteriol. **190:** 7966–7974.
21. **Hegler, F., N. R. Posth, J. Jiang, and A. Kappler.** 2008. Physiology of phototrophic iron(II)-oxidizing bacteria: implications for modern and ancient environments. FEMS Microbiol. Ecol. **66:**250–260.
22. **Johansen, J. R., L. Kováčik, D. A. Casamatta, and J. Kaštovský.** *Leptolyngbya corticola* sp. nov. (*Pseudanabaenaceae*, *Cyanobacteria*), an aerophytic, heteropolar taxon from the Czech Republic. Nova Hedwigia, in press.
23. **Katoh, H., N. Hagino, A. R. Grossman, and T. Ogawa.** 2001. Genes essential to iron transport in the cyanobacterium *Synechocystis* sp. strain PCC 6803. J. Bacteriol. **183:**2779–2784.
24. **Komárek, J., and K. Anagnostidis.** 2005. Cyanoprokaryota. 2. Teil. 2nd part. *Oscillatoriales. In* B. Büdel, L. Krienitz, G. Gärtner, and M. Schagerl (ed.), Süsswasserflora von Mitteleuropa 19/2, p. 759. Elsevier/Spektrum, Heidelberg, Germany.
25. **Komárek, J.** 2007. Phenotype diversity of the cyanobacterial genus *Leptolyngbya* in maritime Antarctica. Pol. Polar Res. **28:**211–231.
26. **Koonin, E. V., and L. Aravind.** 2002. Origin and evolution of eukaryotic apoptosis: the bacterial connection. Cell Death Differ. **9:**394–404.
27. **Larkin, M. A., G. Blackshields, N. P. Brown, R. Chenna, P. A. McGettigan, H. McWilliam, F. Valentin, I. M. Wallace, A. Wilm, R. Lopez, J. D. Thompson, T. J. Gibson, and D. G. Higgins.** 2007. Clustal W and Clustal X version 2.0. Bioinformatics **23:**2947–2948.
28. **Maddison, W., and D. Maddison.** 2003. MacClade 4 software. Sinauer Associates, Sunderland, MA.
29. **Malashenko, I. R., V. A. Romanovskaia, V. N. Bogachenko, and A. D. Shved.** 1975. Thermophilic and thermotolerant bacteria that assimilate methane. Mikrobiologiia **4:**855–862.
30. **Marquardt, J., and K. A. Palinska.** 2007. Genotypic and phenotypic diversity of cyanobacteria assigned to the genus *Phormidium* (*Oscillatoriales*) from different habitats and geographical sites. Arch. Microbiol. **187:**397–413.
31. **McKinney, G.** 1941. Absorption of light by chlorophyll solutions. J. Biol. Chem. **140:**315–322.
32. **Nelissen, B., R. Baere, A. Wilmotte, and R. Wachter.** 1996. Phylogenetic relationships of nonaxenic filamentous cyanobacterial strains based on 16S rRNA sequence analysis. J. Mol. Evol. **42:**194–200.
33. **Olson, J. M., and R. E. Blankenship.** 2004. Thinking about the evolution of photosynthesis. Photosynth. Res. **80:**373–386.
34. **Palinska, K., and J. Marquardt.** 2008. Genotypic and phenotypic analysis of strains assigned to the widespread cyanobacterial morphospecies *Phormidium autumnale* (*Oscillatoriales*). Arch. Microbiol. **189:**325–335.
35. **Papke, R. T., N. B. Ramsing, M. M. Bateson, and D. M. Ward.** 2003. Geographical isolation in hot spring cyanobacteria. Environ. Microbiol. **5:**650–659.
36. **Parenteau, M. N., and S. L. Cady.** 2010. Microbial biosignatures in iron-mineralized phototrophic mats at Chocolate Pots hot springs, Yellowstone National Park, U. S. A. Palaios **25:**97–111.
37. **Pierson, B., M. Parenteau, and B. Griffin.** 1999. Phototrophs in high-iron-concentration microbial mats: physiological ecology of phototrophs in an iron-depositing hot spring. Appl. Environ. Microbiol. **65:**5474–5483.
38. **Pierson, B. K., and M. N. Parenteau.** 2000. Phototrophs in high iron microbial mats: microstructure of mats in iron-depositing hot springs. FEMS Microbiol. Ecol. **32:**181–196.
39. **Prufert-Bebout, L., H. W. Paerl, and C. Lassen.** 1993. Growth, nitrogen fixation, and spectral attenuation in cultivated *Trichodesmium* species. Appl. Environ. Microbiol. **59:**1367–1375.
40. **Saito, M. A., V. Bulygin, D. Moran, E. Bertrand, and J. Waterbury.** 2009. Strategies for economization of iron in *Crocosphaera watsonii* as revealed by global proteomic analyses. Geochim. Cosmochim. Acta **73:**A1145.
41. **Shcolnick, S., T. C. Summerfield, L. Reytman, L. A. Sherman, and N. Keren.** 2009. The mechanism of iron homeostasis in the unicellular cyanobacterium *Synechocystis* sp. PCC 6803 and its relationship to oxidative stress. Plant Physiol. **150:**2045–2056.
42. **Shen, G. Z., and D. A. Bryant.** 1995. Characterization of a *Synechococcus* sp. strain PCC 7002 mutant lacking photosystem I. Protein assembly and energy distribution in the absence of the photosystem I reaction center core complex. Photosynth. Res. **41:**41–53.
43. **Stackebrandt, E., and B. M. Goebel.** 1994. Taxonomic note: a place for DNA-DNA reassociation and 16S rRNA sequence analysis in the present species definition in bacteriology. Int. J. Syst. Bacteriol. **44:**846–849.
44. **Stumm, W., and J. J. Morgan.** 1996. Aquatic chemistry, chemical equilibria and rates in natural waters, 3rd ed., p. 1022. John Wiley and Sons, Inc., New York, NY.
45. **Swofford, D. L.** 1998. PAUP: phylogenetic analysis using parsimony, version 4.02. Sinauer Associates, Sunderland, MA.
46. **Taton, A., S. Grubisic, E. Brambilla, R. De Wit, and A. Wilmotte.** 2003.

Cyanobacterial diversity in natural and artificial microbial mats of Lake Fryxell (McMurdo Dry Valleys, Antarctica): a morphological and molecular approach. Appl. Environ. Microbiol. **69:**5157–5169.

47. **Taton, A., S. Grubisic, P. Balthasart, D. A. Hodgson, J. Laybourn-Parry, and A. Wilmotte.** 2006. Biogeographical distribution and ecological ranges of benthic cyanobacteria in East Antarctic lakes. FEMS Microbiol. Ecol. **57:**272–289.
48. **Wade, M. L., D. G. Agresti, T. J. Wdowiak, L. P. Armendarez, and J. D. Farmer.** 1999. A Mossbauer investigation of iron-rich terrestrial hydrothermal vent systems: lessons for Mars exploration. J. Geophys. Res. **104:**8489–8507.
49. **Widdel, F., S. Schnell, S. Heising, A. Ehrenreich, B. Assmus, and B. Schink.** 1993. Ferrous iron oxidation by anoxygenic phototrophic bacteria. Nature **362:**834–836.
50. **Wilson, C. L., N. W. Hinman, and R. L. Sheridan.** 2000. Hydrogen peroxide formation and decay in iron-rich geothermal waters: the relative of abiotic and biotic mechanisms. Photochem. Photobiol. **71:**691–699.
51. **Zhao, J., G. Shen, and D. A. Bryant.** 2001. Photosystem stoichiometry and state transitions in a mutant of the cyanobacterium *Synechococcus* sp. PCC 7002 lacking phycocyanin. Biochim. Biophys. Acta **1505:**248–257.
52. **Zhu, Y., J. E. Graham, M. Ludwig, W. Xiong, R. M. Alvey, G. Shen, and D. A. Bryant.** Roles of xanthophyll carotenoids in protection against photoinhibition and oxidative stress in the cyanobacterium *Synechococcus* sp. strain PCC 7002. Arch. Biochem. Biophys., in press.